Design of an Optical-access Expansion Chamber for Two-phase Expansion

Steven Lecompte[a], Martijn van den Broek[a], Michel De Paepe[a]

[a]Department of Flow, Heat and Combustion Mechanics, Ghent University, Sint-Pietersnieuwstraat 41, 9000 Gent ,Belgium, steven.lecompte@ugent.be, CA, martijn.vandenbroek@ugent.be ,michel.depaepe@ugent.be

Abstract:

Two-phase expansion processes are seen in various applications and in many cases they allow increasing the overall efficiency of the system. One application is found in LNG liquefaction plants where Joule Thompson valves are replaced with two-phase expanders to increase the overall process efficiency. Among various other examples, also low-temperature thermodynamic power cycles, like the organic Rankine cycle (ORC), benefit from two-phase expansion. However the key challenge is the availability of two-phase expanders. An extensive overview on the knowledge gaps on two-phase expansion is presented in this work. In general, experimental results are scarce and there is no model that can fully predict the expansion process. This is mainly due to the knowledge gap on the fundamental aspects of two-phase expansion and the non-equilibrium effects. Studies based on in-situ flow measurements are solely available for static and circulatory flashing. They however provide a sound basis for a mechanistic process description. Therefore, the concept of a new unique variable volume piston expansion chamber test-rig is described. Preliminary design simulations are performed to evaluate and size the test-rig. The minimum response time of the solenoid valves is flagged as a crucial constraint when sizing the system.

Keywords:

Flash evaporation, Two-phase expansion, Piston expander, Organic Rankine cycle.

1. Introduction

Two-phase expansion processes are seen in various applications and in many cases they allow increasing the overall efficiency of the system. For example, the use of a two-phase expander instead of an expansion valve allows increasing the efficiency of vapour compression cycles (e.g. refrigeration or heat pump units) [1, 2]. Another application is found in LNG liquefaction plants where Joule Thompson valves are replaced with two-phase expanders that generate work and increase the overall process efficiency [3, 4]. Among several other examples, also low-temperature thermodynamic power cycles benefit from two-phase expansion. By omitting full evaporation of the working fluid in an (organic) Rankine cycle, a higher power output can be achieved [5-7]. However the key challenge in this type of cycles, frequently called trilateral cycles (TLC), is the availability of two phase expanders. The adiabatic efficiency of these expanders is a critical parameter which has a large influence on the overall process efficiency.

Technical solutions to two-phase expansion comprise both volumetric and dynamic machines. Early investigated types were the impulse turbine [1] and the twin screw expander [2, 3]. Several challenges were identified for the design of an impulse turbine. Firstly, erosion of the turbine blades should be limited to a suitable selection of material and blade geometry. Secondly, large blade areas are needed to accept the large volume flow rate of the gas; this implies a large shear force between the liquid and the blade. A solution is the use of a multistage turbine to reduce the relative velocity between liquid and blade to reduce the shear force. A main challenge for the twin-screw expander is the relative low built-in volume ratio (between 3 and 9) compared to the actual volume increase over the expander. This results in potentially large under-expansion losses. Increasing the built-in volume ratio however results in relative longer leakage paths and in larger machines for the same mass flow rate. Smith et al. [4] demonstrated that a model with the assumption of a homogeneous one-dimensional flow gives a good prediction of the p-V diagram. This simplification is valid according to the authors because of the considerable rotational component. Considering a

homogeneous flow, the hypothesis is that the liquid part is broken up in sufficient small components which promote a sufficiently mixed flow. The small particles will flash fast to vapour and give rise to an equilibrium temperature between the gas and the liquid phase.

An alternative to the twin-screw expander would be a piston expander. Piston expanders allow for larger built-in volume ratios between 6 and 14 and are thus more adapted to two-phase expansion. The simple geometry furthermore allows for a reduced construction cost. As such, piston type expanders for two-phase flow are readily found in CO_2 refrigeration and CO_2 power systems [5]. A disadvantage of the reciprocating expander is the inherent dead volume that results in some pre-expansion losses. There is also the complexity associated to actuating and timing the inlet and outlet valves. As there is no direct rotational component, it is furthermore unclear whether the assumption of an equilibrium homogeneous flow is still valid. When looking for example to static flashing, see further in section 2.1, there are clearly non-equilibrium effects. Fortunately, the geometry of the piston expanders lends itself to in-situ flow measurements. The process of the two-phase expansion can thus be experimentally examined and mechanistic models can be validated. To the authors' knowledge there is, alas, no prior research on this topic.

In this work, the two-phase flashing process will be discussed first. Next, an overview is given of the different models which allow predicting the non-equilibrium effects of two-phase flashing. The model parameters and needed constitutive equations are compared. This gives the reader a grasp of the level of complexity and the challenges for each of the different modelling choices. Finally, an initial design of an optical accessible two-phase piston expander is proposed. An approximate model is presented and the results are discussed.

2. Two-phase flashing process

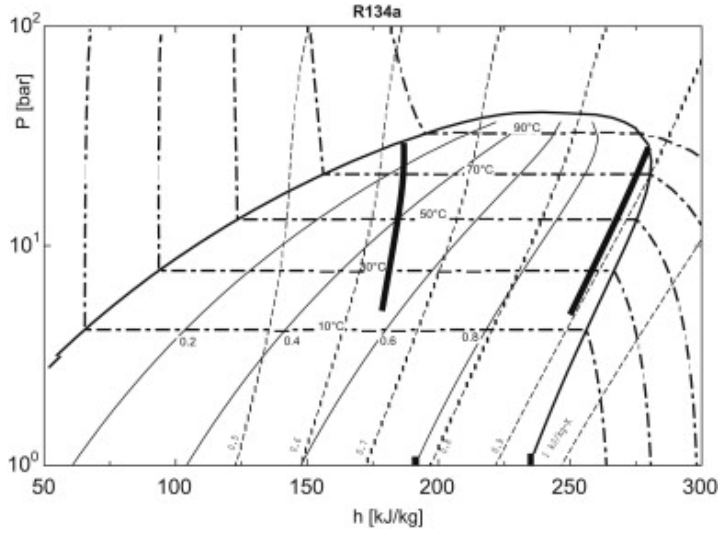

Fig. 1. Use of appropriate contrasted colours for black and white printing: a) colour figure, b) greyscale figure.

The expected behaviour of the continuous two-phase expansion process, see Figure 1, is that the working fluid flashes into a liquid-vapour mixture. This system is in a non-equilibrium state because of the difference in temperature and velocity between the two phases [6, 7]. The vapour fraction can be considered to enter as saturated vapour and during expansion, the vapour becomes partly subcooled before being condensed. The liquid fraction on the other hand partly evaporates during expansion. The rate of evaporation changes according to the number of nuclei during the boiling and the superheat of the liquid. However, the behaviour is more complex as one can expect an interaction between the gaseous and the liquid state because of the good thermal contact between the two-phases [6]. This interaction ultimately results in a net vapour generation rate per unit volume during flashing that can be expressed as [7, 8]:

$$\dot{m}_{ev} = \frac{A_i \dot{q}_i}{h_{lg}}. \quad (1)$$

With A_i the liquid-vapour interfacial area, $\dot{q}_i$ the net heat flux to the interface and h_{lg} the latent heat of evaporation.

2.1. Static flash

Flash evaporation has mostly been studied for constant volume chambers under a gradual pressure decrease. This type of evaporation is labelled as static flashing. The important external parameters in this case are the initial liquid level and the depressurization rate [9]. Studies on flash evaporation in constant volume chambers investigate the vapour generation rate and the flashing time. Several empirical 0D models were proposed [10-15]. The non-equilibrium fraction (NEF) was introduced by Miyatake et al. [16, 17] to comprehensively describe the flash evaporation process:

$$NEF = \frac{T - T_e}{T_0 - T_e}, \quad (2)$$

with T_0 the initial temperature of the liquid, T_e the equilibrium temperature of the liquid and T the temperature at a certain time. The NEF will be equal to one at the start of flashing and zero at the end of the flashing process. The NEF can also be written in function of m_{ev} (eq. 4). Consider a global energy balance; the energy of vaporization is taken from the liquid cooling, the volume of liquid after flashing is taken equal to the initial water mass and the fluid properties are taken as constant. The value of m_{ev} can then be written as [11]:

$$m_{ev} = \frac{\rho_l V_0 c_{p,l}}{h_{lg}} (T_0 - T), \quad (3)$$

this allows writing the NEF as:

$$NEF = \frac{m_{ev,e} - m_{ev}}{m_{ev,e}}. \quad (4)$$

The NEF thus gives a direct measure for the mass of fluid evaporated. The trend of the NEF in function of time typically shows two distinct parts. First, there is a strong reduction in NEF corresponding to intense boiling followed by an asymptotic decrease to zero corresponding to gradual evaporation of the liquid. Both parts show an exponential decay. Empirical correlations have been developed to predict m_{ev} [10-12]. These correlations take the important initial conditions of liquid superheat, depressurization rate and liquid height as input parameters. Fitting coefficients are then matched to the experimental datasets. However, as also Saury and Siroux [11] note, it would be interesting to analyse fundamental aspects of the bubble formation in order to predict in a mechanistic way the evaporated mass. As such, the physical aspects at the interfacial area between liquid and vapour needs to be investigated.

2.2. Circulatory flash

In contrast to static flash, the liquid film in circulatory flash has a nonzero velocity. This is sometimes named a flashing flow. The main application is found in desalination plants which incorporate multi-stage flash (MSF) distillation [18, 19]. A continuous flow of liquid brine enters successive flashing chambers where the water is flashed and subsequently condensed in order to separate the salt. Again, phenomenological correlations are used to predict the mass of liquid evaporated. Junjie et al. [15] considers the concept of an overall heat transfer coefficient to model the heat transfer between the liquid and the vapour phase. This heat transfer coefficient is a time dependent function.

Yet, few studies look at the physical aspects at the interfacial area. Saha et al. [8] note that both A_i and $\dot{q}_i$ in eq. 1 are flow-regime-dependent and are functions of the thermodynamic states and flow variables. Based on the void fraction, they divide the flow in bubbly flow, bubbly-slug flow, annular and annular mist flow. Several suitable void fraction correlations are summarized in the paper of Mayinger [20]. More recently Pinhasi et al. [21] used a similar method to model the blowdown of pressure liquefied gases from a vessel. This modelling approach is supported by the

statement of Mayinger et al [20]. They proclaim that phase separation models that analyse the rising velocity of one bubble are generally unsuccessful; the phase separation is better expressed by means of the void fraction profile.

The modelling approach by Saha et al. [8] is analogous to the current state of the art in solving two-phase flows in heat exchangers with the help of flow maps [22-24]. Yet, limited experimental research is available on the void fraction profile and the flow maps during flashing [25, 26]. For variable volume flashing, it is even worse as no data is available.

2.3. Variable volume flash

Besides systems where either the liquid is static or is flowing, there are systems where the volume of the flashing chamber changes during time. Obvious examples are two-phase volumetric expanders. The volumetric displacement is described by the equations of motion. The change in volume will influence the pressure in the system and affect the dynamics of the flashing.

Kanno et al. [7] is one of the few authors who investigate flashing in a variable volume chamber. An experimental setup mimicking a two-phase reciprocating expander was built. Instead of working with an actual high pressure inlet, the flashing is induced under vacuum pressure by the work of a linear actuator. Their developed model was greatly simplified by lumping the non-equilibrium effects in the boiling phenomena with an agitation factor β. The factor β essentially replaces the parameter A_i in eq. 1. This agitation factor is fitted to experimental data to predict the pressure in the system. This gives good results but this tells us nothing about the physical behaviour at the interfacial area and the actual distribution of the vapour and liquid phase. The model is therefore difficult to generalize to new conditions like other fluids, geometries or different starting pressures and temperatures without recalibration.

3. Two-phase flashing models

In this section, an overview is given of the two-phase models which allow predicting the flashing process.

3.1. Two-fluid model

The two-fluid model depicts the most general multiphase description in this overview. A detailed discussion can be found in the book of Johnson [27]. Each phase is considered as a separate fluid with its own set of conservation equations. As such, each phase has its own velocity, pressure and temperature. The temperature difference is basically induced by heat transfer phenomena between the phases. If there are rapidly changing flow conditions, the time lag for reaching thermal equilibrium between the phases may become significant. This will be the case for the flashing flows described above. Besides the mass, energy and momentum balance for the different phases additional constitutive equations are necessary:

$$\dot{q}_i = h_i(T_1 - T_2), \quad (5)$$

$$p_1 = p_2 \quad (6)$$

$$\dot{m}_1 = -\dot{m}_2 = \text{f(fluid properties)}, \quad (7)$$

$$\frac{A_i}{L_i} = \text{f(flow regime)}, \quad (8)$$

in these equations, $\dot{q}_i$ is the heat transfer per unit area, $\frac{A_i}{L_i}$ the characteristic interfacial area per unit length and h_i the characteristic interfacial heat transfer correlation. The time scale of a pressure in-equilibrium is assumed to be much lower than that of the expansion process (eq. 6). The evaporated mass can be determined from the fluid properties (latent heat), the heat transfer coefficient h_i and the interfacial area A_i. The challenge lies in developing accurate and general correlations for A_i and h_i. A mechanistic model, based on the fluid dynamics of the boiling during flashing, is therefore essential. However this implies detailed modelling and foremost an extensive experimental campaign which allows calibrating all the necessary constants in the empirical closure equations.

3.2. Homogeneous equilibrium model

The homogeneous equilibrium model (HEM) is a simplification of the two-fluid model where one assumes that the velocity, pressure and temperature are given for one averaged pseudo-fluid. The equation of state for this pseudo-fluid now associates the two phases. It is clear from experiments on static, circulatory and variable volume flashing that the assumption of an equilibrium velocity or temperature is not valid. As such, this model is not very suitable to investigate the flashing process in this work. In general, it is stated that any large driving potential relative to the reference state voids the equilibrium hypothesis [27].

3.3. Homogenous relaxation model

The homogeneous relaxation model (HRM) provides a mathematical straightforward alternative for the two-fluid model. Considering the two-phase expansion process, flashing starts with some delay and the slip between the two phases can be assumed of secondary importance to the non-equilibrium effects. The homogeneous relaxation model thus consists of the same basic equations as the HEM model but with the addition of a relaxation equation to model the vapour generation rate. Bilicki and Kestin [28] relate the relaxation equation to the vapour fraction x of the fluid according to the form:

$$\frac{\partial x}{\partial t} = \frac{\dot{m}_{ev}}{\rho} = -\frac{x - x_{eq}}{\theta}. \quad (9)$$

As there is no analytical closure term, the instantaneous relaxation time θ is experimentally determined. Due to the dependency on empirical data, the applicability of these correlations is thus confined to the conditions reported during the experiments. A well-known set of experiments are the 'Moby Dick' experiments [29]. In these experiments a blowdown test with water was performed through a conical divergent nozzle. The mass flow rate, the pressure and void fraction distribution were measured in the longitudinal direction during the expansion process. For small pressures (up to 10 bar) the following correlation was proposed by Downar-Zapolski et al.:

$$\theta = 6.51 \times 10^{-4} \left(\frac{p_0 - p}{p_0}\right)^{-0.257} \left(\frac{x v_{sg}}{v}\right)^{-2.24} \quad (10)$$

In this equation, p_0 is the saturation pressure at the inlet temperature,v the specific volume and v_{sg} the specific volume at saturated vapour. Note that the instantaneous relaxation time depends on the current value of the vapour fraction x. For larger pressures an alternative correlation was suggested.

A similar set of equations for $C0_2$ was obtained by Angielczyk et al. [30]. An apparent step in generalizing the above model is introducing a mechanistic model of the bubble growth and the corresponding heat transfer with the superheated liquid [31]. This increased level of complexity can however lead to the same challenges as with two-fluid models.

4. Variable volume piston expansion chamber

In order to investigate variable volume flashing, a test rig will be built at the Applied Thermodynamics & Heat Transfer (ATHT) lab. This test rig will be based on the one of Kanno et al. [7]. However, there are several key adaptations required to reflect real operational regimes. In contrast, the new test rig will be designed to work under high temperatures (<160 °C) and pressures (<15 bar). Furthermore the design allows working with established ORC fluids. The processing of the data will be done using an adapted version of the HRM. Instead of working with a single correlation to determine the relaxation time θ, flow-regime-dependent correlations will be proposed to improve accuracy. Several authors [8, 20, 21] use detailed flow-regime dependent models to describe flashing flows, but this has never been applied to the HRM.

To investigate the effect of different working fluids, cyclopentane is chosen as secondary fluid besides water. Contrary to water, cyclopentane does not result in the expected under expansion losses predicted by 0D models [32, 33]. Furthermore, the use of water gives an under pressure in the condenser this results in a more complex system that needs vacuum equipment. Cyclopentane is

already used commercially in subcritical ORC installations by Atlas Copco [34], General-Electric [35] and Turboden [36]. In addition, there is abundant information available on the thermophysical and transport properties [37-40]. Still, water is the reference fluid of choice for investigating flashing due to the availability of previous research. As cyclopentane is not compatible with rubbers and polystyrene, these materials are avoided in the design.

In order to size the expansion chamber, a simulation based on the HEM has been developed. The HEM will give an over assumption of the pressures in the cylinder. Considering that this is a design model and that there is no previous research available to accurately implement the non-equilibrium effects this is deemed acceptable.

4.1. Nominal design and test rig

The layout of the test-rig is shown in Figure 2. The piston diameter is 30 mm; the piston and cylinder assembly is partly in glass (quartz) and stainless steel [41, 42]. The mechanical load is provided by an electromechanical linear actuator. Solenoid valves are used as the inlet and outlet valves. The working fluid is heated in a shell and tube heat exchanger wherein the secondary flow is heated by a thermal oil loop. The nominal design parameters are listed in Table 1.

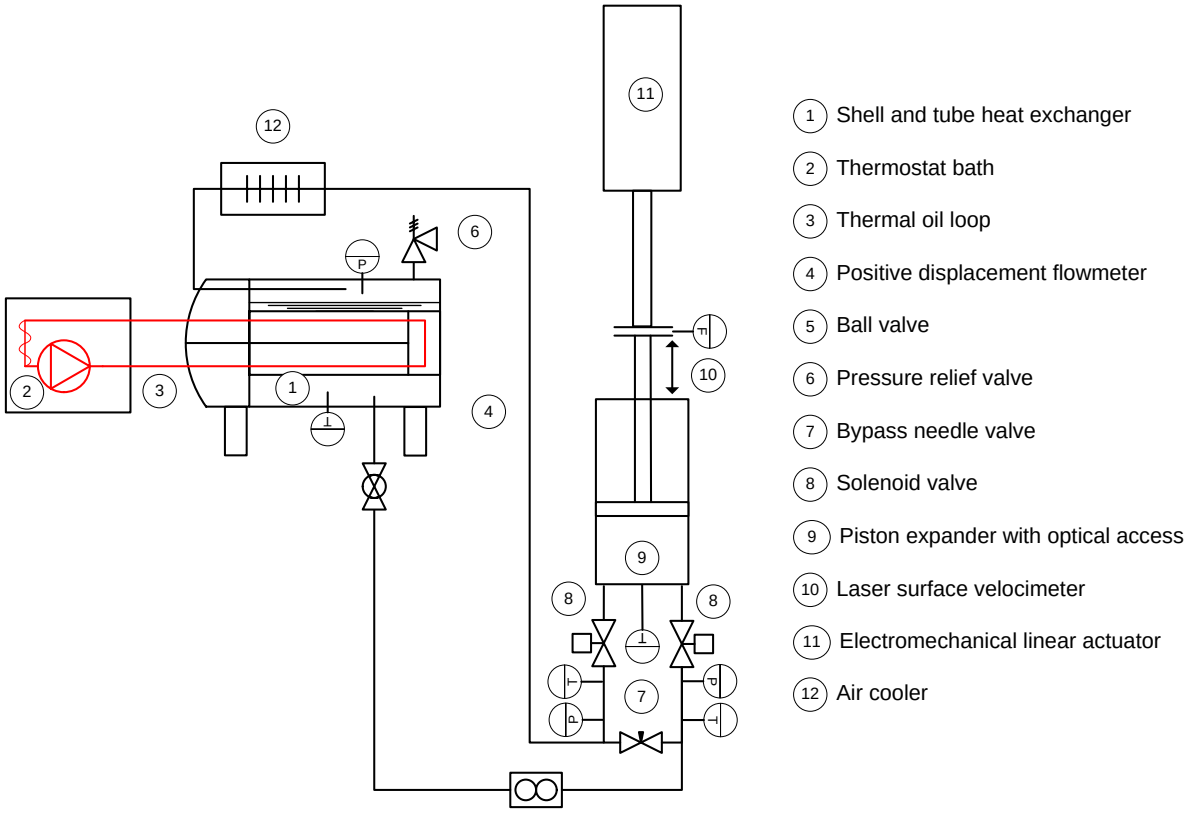

Fig. 1. Preliminary layout of the test-rig

Table 1. Nominal design values.

Design parameter	*Value*	*Unit*
Piston bore	30	mm
Piston maximum stroke	400	mm
Minimum valve response time	10	ms
Valve orifice	4.76	mm
Maximum force on piston	1.06	kN
Material piston	Quartz (piston crown) and stainless steel with graphite sealing	
Material cylinder	Quartz and stainless steel	
Working fluids	Water and cyclopentane	

4.2. Design equations

The dynamics of the piston motion is described by Newton's second law:

$$m_p\left(\frac{d^2x}{dt^2}\right) = \frac{\pi D_{cyl}^2}{4}\left(p_{cyl} - p_{bp}\right) - F_{fr} - F_{load}, \quad (11)$$

with p_{cyl} the instantaneous pressure inside the cylinder and p_{bp} the pressure at the outside of the piston which is equal to atmospheric pressure. F_{fr} is the friction force between piston and cylinder wall and F_{load} the external load from the electromechanical linear actuator. The expansion process is modelled as a sequence of small equilibrium steps: an isentropic expansion, isochoric heating by friction and heat transfer from or to the expander walls. The heat transfer from the walls is expressed as:

$$\dot{Q}_{cyl} = h_{wall}.A_{wall}.\left(T_{cyl} - T_{wall}\right). \quad (12)$$

For the cylinder surface temperature T_{wall}, the average between inlet and outlet conditions is taken as:

$$T_{wall} = \frac{T_{in} - T_{out}}{2}. \quad (13)$$

For this type of application, the Woschni [43] heat transfer correlation is chosen as suggested by Gusev et al. [44]:

$$h = 3.26D^{-0.2}{p_{cyl}}^{0.8}{T_{cyl}}^{-0.55}\left(\frac{dx}{dt}\right)^{0.8}. \quad (14)$$

The friction force F_{fr} is modelled assuming the behaviour of pneumatic cylinders. As described by Tran and Yanada [45] an adapted LuGre model is implemented.

The working fluid enters the expander through an orifice in the solenoid valve. The mass flow rate trough this valve is modelled by assuming steady-state, incompressible, inviscid, laminar flow:

$$\dot{m} = C.A_{or}.\sqrt{2\rho_{in}\left(p_{in} - p_{cyl}\right)} \quad (15)$$

The flow coefficient C of 0.430 and the orifice diameter of 4.67 mm is taken from the datasheet of the manufacturer [46].

4.3. Simulation results and discussion

Two cases, corresponding to the two working fluids, are investigated. Both water and cyclopentane enter the expander as saturated liquid. The clearance volume (i.e. dead volume) includes all crevices and allows for a safety distance between piston and cylinder head. The boundary conditions can be found in Table 2. These conditions correspond to the upper operating range of the test-rig. The aim is to assess the design constraints of the system. These include maximum acceleration, maximum velocity and effect of the inlet timing.

Table 2. Simulation boundary values.

Simulation value	*Value*	*Unit*
Inlet pressure		
Water	4.761	bar
Cyclopentane	11.96	bar
Inlet temperature		
Water	150	°C
Cyclopentane	150	°C
Clearance volume	5	% of the total displacement volume
Load profile	$50.V^2$	N
Piston weight	2	kg
Valve response time (open + close)	20	ms

In the current design, the electromechanical actuator will be used to push out the working fluid after expansion. As such, the p-V diagram for water as working fluid looks like Figure 2a. On the other

hand, if the remaining working fluid is kept at a condition equal to the end of expansion, the p-V diagram looks like Figure 3. In this case, there is a pre-expansion which fills the clearance volume. For simplicity, the remainder of the analysis is done with the electromechanical actuator pushing the working fluid out. Due to the relative slow closing and opening of the solenoid valve and the small orifice, there is already a pressure reduction in the cylinder during filling. The piston stroke to bore ratio should preferably be low to reduce friction and heat losses. A fast intake process, resulting in a low intake mass, is thus beneficial considering the high specific volume increase during expansion. Going to a larger orifice thus necessitates a faster valve to reduce the inlet mass. However, a larger orifice and a faster response time lead to a larger electrical coil for actuating the valve. Unfortunately, this type of equipment is not commercially available. Figure 2b and 2c show respectively the velocity and the acceleration of the piston. Important for the design, is that both the maximum velocity and the maximum acceleration fall in the operating range of an electromechanical linear actuator.

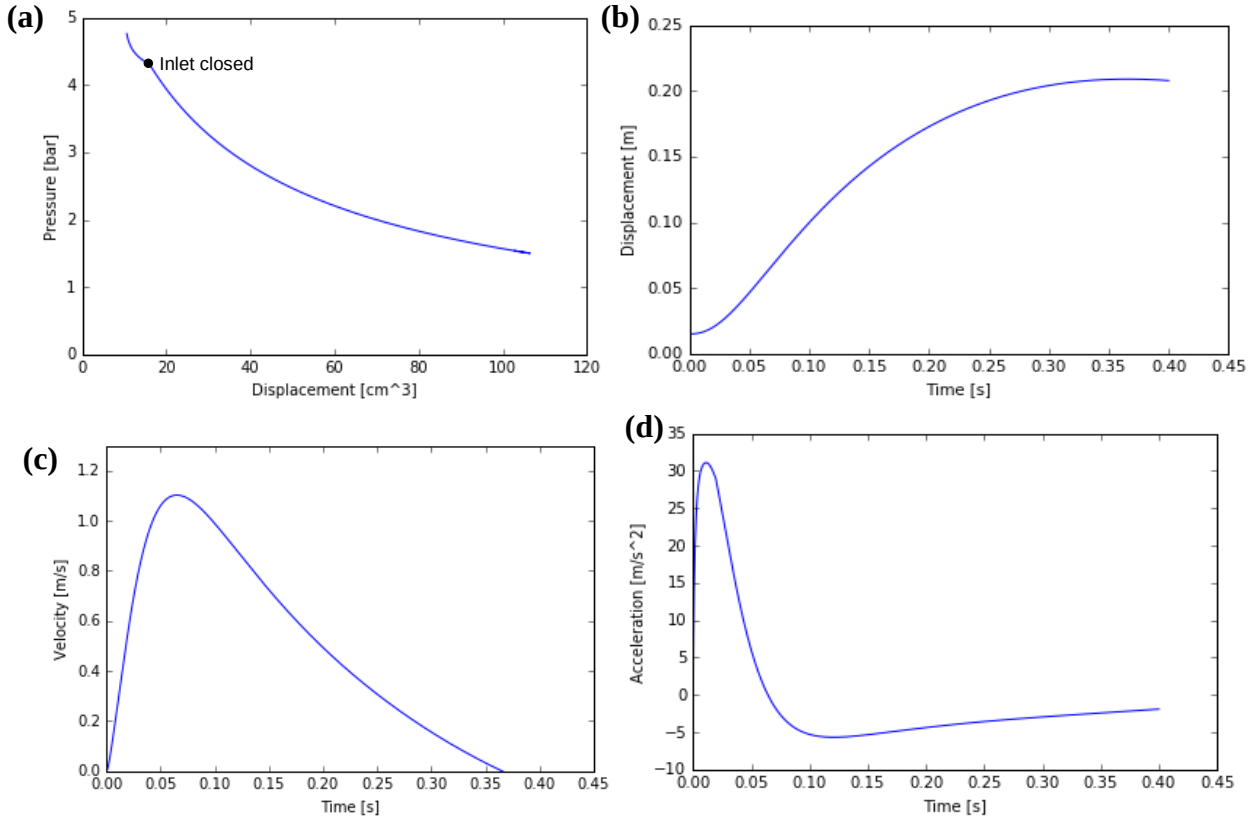

Fig. 2. a) p-V diagram, b) piston displacement, c) piston velocity, d) piston acceleration in function of time for the working fluid water.

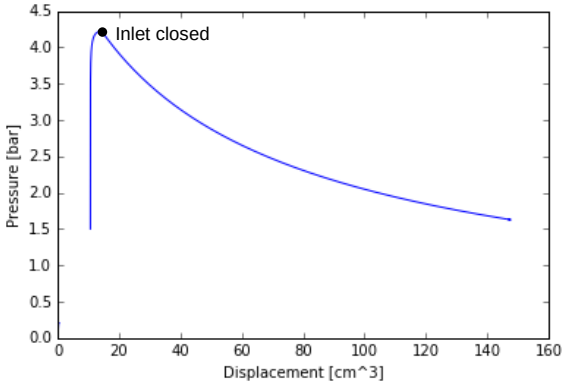

Fig. 3. p-V diagram (water) with clearance volume at condition corresponding with the end of expansion.

The same design and operating conditions are investigated for the working fluid cyclopentane. At the same inlet temperature of 150°C the saturation pressure is now increased to 11.96 bar. The corresponding results can be found in Figure 4. The maximum displacement is now increased to 0.392 m, the maximum velocity to 2.36 m/s and the maximum acceleration to 145 m/s². These values are still within range for a design with an electromechanical linear actuator. Note that in this case the pre-expansion during the inlet stage is more pronounced. A faster valve, with larger inlet orifice, would certainly be valuable in this instance. An important benefit of working with cyclopentane, is that the average power output is increased significantly from 97.7W for water to 216.0W and this for the same inlet temperature of the saturated working fluid.

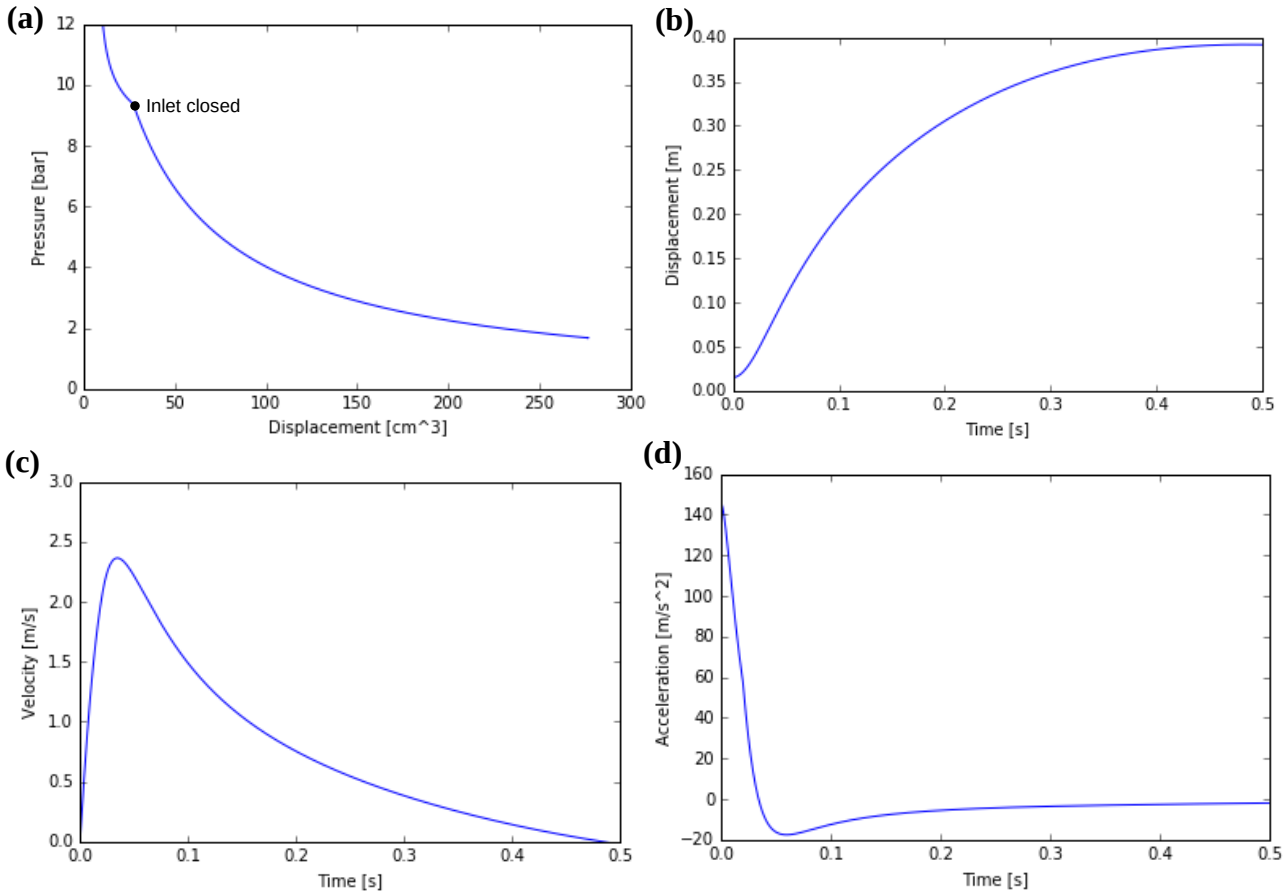

Fig. 4. a) p-V diagram, b) piston displacement, c) piston velocity, d) piston acceleration in function of time for the working fluid cyclopentane.

5. Conclusions

A comprehensive overview on the state of the art in two-phase flashing processes was compiled in this work. From this overview, it is immediately clear that mostly static and circulatory flashing are investigated. Flashing in a pressure chamber with changing volume (i.e. variable volume flashing) is almost not examined in literature, despite their relevance in two-phase volumetric expanders. Yet, the modelling principles used in static and circulatory flashing are useful to describe variable volume flashing.

Three two-phase models are elaborated which have the potential to describe flashing. The two-fluid model is the most general but relies heavily on empirical constitutive relations to model interfacial effects. These constitutive correlations are complicated to acquire from experimental results. The homogeneous equilibrium model (HEM) is simple but is not suitable to accurately describe flashing. Finally, there is the homogeneous relaxation model (HRM) which offers a straightforward framework to describe flashing from experimental data. It also has the potential for increased accuracy by making the necessary empirical correlations flow-regime dependent.

All the models depicted above depend on empirical data. Therefore the design of a unique reciprocating test rig was presented. The mechanical load is provided by an electromagnetic linear actuator. The bore of the piston is 30 mm and the maximum stroke 400 mm. Solenoid valves are used as inlet and outlet valves. The maximum inlet pressure and temperature is respectively 15 bar and 160 °C. Both cyclopentane and water will be investigated as working fluid. The first simulations indicate the need for fast acting valves. The solenoid valves are relatively slow and small and constrain the size of the piston-cylinder assembly. The simulations also confirm that both maximum piston velocity and acceleration fall within the range of a linear electromechanical actuator.

Acknowledgments

The research for this paper was funded by Ghent University (BOF16/PDO/061). This support is gratefully acknowledged.

Nomenclature

A	area, m²
c_p	specific heat, J/(kg K)
F,	force, N
h_{lg}	latent heat, J/kg
L	length, m
m	mass, kg
$\dot{m}$	mass flow rate, kg/s
p	pressure, pa
$\dot{q}$	net heat flux per unit area, W/m²
v	specific volume, m³/kg
x	vapour fraction, -

Greek symbols

θ	relaxation time, s
ρ	density, kg/m³

Subscripts and superscripts

0	initial starting values
cyl	cylinder
e	equilibrium
i	interface liquid-vapour
sg	saturated vapour
sl	saturated liquid

References

[1] G.E. David. Theory and Tests of Two-Phase Turbines. in: U.S Department of Energy, (Ed.).1982. p. 149.
[2] R.F. Steidel, H. Weiss, J.E. Flower. Performance Characteristics of the Lysholm Engine as Tested for Geothermal Power Applications in the Imperial Valley. in: Lwarence Livermore Laboratory, (Ed.).1977.
[3] R. McKay. Helical Screw Expander Evaluation Project. in: U.S.D.o. Energy, (Ed.).1982. p. 458.

[4] I.K. Smith, N. Stosic, C.A. Aldis. Development of the trilateral flash cycle system Part3: the design of high-efficiency two-phase screw expanders. Proceedings of the Institution of Mechanical Engineers, Part A: Journal of Power and Energy. (1996).
[5] J.S. Baek, E.A. Groll, P.B. Lawless. Piston-cylinder work producing expansion device in a transcritical carbon dioxide cycle. Part I: experimental investigation. International Journal of Refrigeration. 28 (2005) 141-51.
[6] H. Öhman, P. Lundqvist. Experimental investigation of a Lysholm Turbine operating with superheated, saturated and 2-phase inlet conditions. Applied Thermal Engineering. 50 (2013) 1211-8.
[7] H. Kanno, N. Shikazono. Experimental and modeling study on adiabatic two-phase expansion in a cylinder. International Journal of Heat and Mass Transfer. 86 (2015) 755-63.
[8] P. Saha, N. Abuaf, B.J.C. Wu. A Nonequilibrium Vapor Generation Model for Flashing Flows. Journal of Heat Transfer. 106 (1984) 198-203.
[9] D. Zhang, J. Yan, Y. Liu, B. Zhao. Preliminary exergy analysis of static flash of pure water. International Journal of Heat and Mass Transfer. 86 (2015) 377-87.
[10] S. Gopalakrishna, V.M. Purushothaman, N. Lior. An experimental study of flash evaporation from liquid pools. Desalination. 65 (1987) 139-51.
[11] D. Saury, S. Harmand, M. Siroux. Flash evaporation from a water pool: Influence of the liquid height and of the depressurization rate. International Journal of Thermal Sciences. 44 (2005) 953-65.
[12] D. Saury, S. Harmand, M. Siroux. Experimental study of flash evaporation of a water film. International Journal of Heat and Mass Trasnfer. 45 (2002) 10.
[13] O. Miyatake, T. Fujii, T. Tanaka, T. Nakaika. Flash evaporation phenomena of pool water. Heat Transfer Japan. 6 (1977) 12.
[14] O. Miyatake, Y. Murakami, Y. Kawata, T. Fujii. Fundamental experiments with flash evaporation. Heat Transfer Japan. 2 (1973) 11.
[15] Y. Junjie, Z. Dan, C. Daotong, W. Guifang, L. Luning. Experimental study on static/circulatory flash evaporation. International Journal of Heat and Mass Transfer. 53 (2010) 5528-35.
[16] O. Miyatake, K. Murakami, Y. Kawata, T. Fujii. Fundamental experiments with flash evaporation. Heat Transfer - Japanese Research. 2 (1973) 89-100.
[17] O. Miyatake, T. Fujii, T. Tanaka, T. Nakaoka. Flash evaporation phenomena of pool water. Heat Transfer - Japanese Research. 6 (1977) 13-24.
[18] W.X. Jin, S.C. Low. Investigation of single-phase flow patterns in a model flash evaporation chamber using PIV measurement and numerical simulation. Desalination. 150 (2002) 51-63.
[19] W.X. Jin, S.C. Low, S.C.M. Yu. Some experimental observations on the single and multi-phase flow patterns in a model flash evaporation chamber. International Communications in Heat and Mass Transfer. 26 (1999) 839-48.
[20] F. Mayinger. Two-Phase Flow Phenomena with Depressurization - Consequences for the Design and Layout of Safety and Pressure Relief Valves. Chem Eng Process. 23 (1987) 11.
[21] G.A. Pinhasi, A. Ullmann, A. Dayan. 1D plane numerical model for boiling liquid expanding vapor explosion (BLEVE). International Journal of Heat and Mass Transfer. 50 (2007) 4780-95.
[22] N. Kattan, J.R. Thome, D. Favrat. Flow Boiling in Horizontal Tubes: Part 1—Development of a Diabatic Two-Phase Flow Pattern Map. Journal of Heat Transfer. 120 (1998) 140-7.
[23] N. Kattan, J.R. Thome, D. Favrat. Flow Boiling in Horizontal Tubes: Part 2—New Heat Transfer Data for Five Refrigerants. Journal of Heat Transfer. 120 (1998) 148-55.
[24] A. Manera, H.M. Prasser, D. Lucas, T.H.J.J. van der Hagen. Three-dimensional flow pattern visualization and bubble size distributions in stationary and transient upward flashing flow. International Journal of Multiphase Flow. 32 (2006) 996-1016.
[25] L. Friedel, S. Purps. Phase distribution in vessels during depressurisation. International Journal of Heat and Fluid Flow. 5 (1984) 229-34.
[26] B. Gebbeken, R. Eggers. Blowdown of carbon dioxide from initially supercritical conditions. Journal of Loss Prevention in the Process Industries. 9 (1996) 285-93.

[27] R.W. Johnson. Handbook of Fluid Dynamics, Second Edition. CRC Press2016.
[28] P. Downar-Zapolski, Z. Bilicki, L. Bolle, J. Franco. The non-equilibrium relaxation model for one-dimensional flashing liquid flow. International Journal of Multiphase Flow. 22 (1996) 473-83.
[29] M. Reocreux. Contribution a l'etude des debits critiques en ecoulement diphasique eau-vapeur. Université Scientifique et Medicale de Grenoble,1974.
[30] W. Angielczyk, Y. Bartosiewicz, D. Butrymowicz, J.-M. Seynhaeve. 1-D modeling of supersonic carbon dioxide two-phase flow through ejector motive nozzle. (2010).
[31] Z. Bilicki, R. Kwidziński, S.A. Mohammadein. Evaluation of the relaxation time of heat and mass exchange in the liquid-vapour bubble flow. International journal of heat and mass transfer. 39 (1996) 753-9.
[32] S. Lecompte, M. van den Broek, M. De Paepe. Performance potential of ORC architectures for waste heat recovery taking into account design and environmental constraints. 3rd International Seminar on ORC Power Systems, Brussels, Belgium, 2015.
[33] J. Fischer. Comparison of trilateral cycles and organic Rankine cycles. Energy. 36 (2011) 6208-19.
[34] Atlas Copco. Brochure: Delivering complete ORC solutions. 2015.
[35] A. Burrato. ORegen Waste Heat Recovery: Development and Applications. 2nd International Seminar on ORC Power Systems, Rotterdam, 2013.
[36] Chetwynd 12 MW power project, www.nec-bc.ca/projects/chetwynd-12-mw-power-project, Last accessed: 14 January 2016.
[37] T.H. Chung, M. Ajlan, L.L. Lee, K.E. Starling. Generalized multiparameter correlation for nonpolar and polar fluid transport properties. Industrial & Engineering Chemistry Research. 27 (1988) 671-9.
[38] C.-M. Vassiliou, M. Assael, R. Perkins. Reference Correlations of the Thermal Conductivity of Cyclopentane, iso-Pentane, and n-Pentane. Journal of Physical and Chemical Reference Data. 44 (2015).
[39] H. Gedanitz, M.J. Davila, E.W. Lemmon. Speed of Sound Measurements and a Fundamental Equation of State for Cyclopentane. Journal of Chemical & Engineering Data. 60 (2015) 1331-7.
[40] A. Mulero, I. Cachadiña. Recommended Correlations for the Surface Tension of Several Fluids Included in the REFPROP Program. Journal of Physical and Chemical Reference Data. 43 (2014) 023104.
[41] S. Buhl, F. Gleiss, M. Köhler, F. Hartmann, D. Messig, C. Brücker, et al. A combined numerical and experimental study of the 3D tumble structure and piston boundary layer development during the intake stroke of a gasoline engine. Flow, Turbulence and Combustion. (2016) 1-22.
[42] C. Espey, J.E. Dec. Diesel engine combustion studies in a newly designed optical-access engine using high-speed visualization and 2-D laser imaging. SAE Technical Paper1993.
[43] G. Woschni. A Universally Applicable Equation for the Instantaneous Heat Transfer Coefficient in the Internal Combustion Engine. SAE Technical Paper. (1967).
[44] S. Gusev, D. Ziviani, J. De Viaene, S. Derammelaere, M. van den Broek. Modelling and preliminary design of a variable-BVR rotary valve expander with an integrated linear generator. 23rd International Compressor Engineering Conference, Purdue University, West Lafayette, USA, 2016.
[45] X.B. Tran, H. Yanada. Dynamic friction behaviors of pneumatic cylinders. Intelligent Control and Automation. 4 (2013).
[46] Gemssensors B-series valve, URL: http://www.gemssensors.com/~/media/GemsNA/NEW%20CATALOG%20FILES%20-%202013/2015%20updates/B-Series-Valves-25-FEB-15.ashx, Last accessed: 3/02/2017.